ChemPubSoc Europe

DOI: 10.1002/chem.201501254

CHEMISTRY A European Journal Full Paper

Porphyrinoids

Synthesis and Atropisomerism of Cascaded Tetraphenylporphyrin–[60]Fullerene Hybrids

Sebastian Schlundt, Walter Bauer, and Andreas Hirsch*[a]

Abstract: Flexible, linked dendritic tetraphenylporphyrin (TPP)–fullerene hybrids were synthesized. They were designed to gain insight into and mimic the primary events in the natural photosynthetic reaction center. These multiporphyrin moieties are based on a light-harvesting concept. Moreover, they incorporate multiple redox components aligned along a redox gradient. Newkome-type dendrons were added to these TPP–fullerene hybrids. In principle they can mediate pH-dependent water solubility, which, however, could not be observed in this case. A protecting-group strategy using *tert*-butyldiphenylsilyl groups allows convergent synthesis of the dendritic compounds. The dendritic multiporphyrins were synthesized separately and can be used as individual building blocks. Atropisomerism was observed in the dendritic compounds, and single atropisomers could be assigned to the corresponding peaks of a characteristic pattern in the NMR spectra. Deprotection of the Newkome-type dendrons was shown to be feasible under mild conditions that leave the redox gradient intact.

Introduction

Porphyrin–fullerene conjugates are capable of photoinduced electron transfer and thus can act as synthetic analogues of natural photosynthesis. The conjugates can be incorporated in an extended linear redox gradient to enhance their ability for photoinduced electron transfer. Extended linear redox gradients were used by Imahori and co-workers[1–6] and Guldi and co-workers.[7] The conjugates can also be part of a dendritic molecule to improve light harvesting due to multiple chromophores, which was shown by Gust and co-workers[8] and by Ito and coworkers.[9] We have contributed porphyrin–fullerene dyads,[10,11] water-soluble dyads,[12–14] and dendritic TPP–fullerene conjugates (Figure 1).[15] Herein, we report the extension of our previously reported dendritic TPP–[60]fullerene hybrid **1**[15] (Figure 1) by ferrocene, which resulted in conjugate **2** (Figure 2). Compared to compound **1**, conjugate **2** has potentially improved ability for photoinduced electron transfer due to its larger dendritic gradient (C_{60}-H_2P-ZnP-Fc; H_2P = free-base porphyrin, ZnP = zinc porphyrin, Fc = ferrocene). Here we emphasize the synthesis and characterization of our compounds. The architecture of **1** and **2** is summarized as Prototype I (Figure 3).

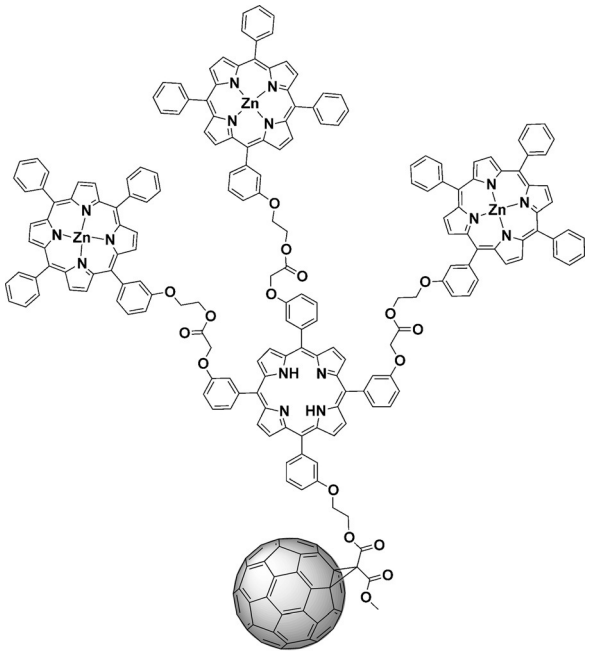

1

Figure 1. $(ZnP)_3$-H_2P-C_{60} **1**,[15] affiliated with Prototype I.

[a] *S. Schlundt, W. Bauer, Prof. Dr. A. Hirsch*
Department of Chemistry and Pharmacy &
Interdisciplinary Center of Molecular Materials (ICMM)
Friedrich-Alexander-Universität Erlangen-Nürnberg
Henkestrasse 42, 91054 Erlangen (Germany)
Fax: (+49) 9131-852-6864
E-mail: andreas.hirsch@fau.de

Supporting information for this article is available on the WWW under http://dx.doi.org/10.1002/chem.201501254.

We also report extension of our dendritic conjugate **1** by Newkome-type dendrons, which results in compounds **3** and **4** (Figure 4). Conjugate **3** can be deprotected to generate free carboxyl groups (compound **4**), which are in principle able to mediate water solubility. Compounds **3** and **4** are symbolized as Prototype II (Figure 5). During the course of the synthesis of our new TPP moieties we noted interesting atropisomerism phenomena using NMR spectroscopy. Herein, we report in

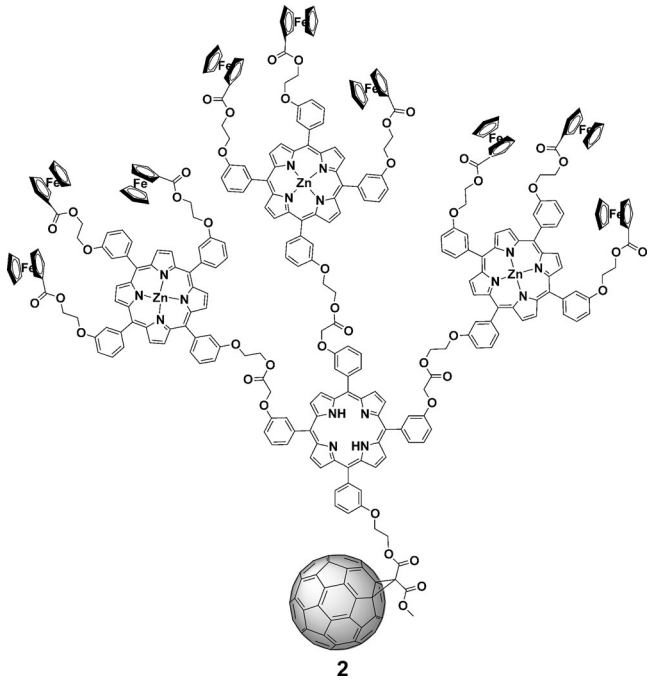

Figure 2. Fc_9-$(ZnP)_3$-H_2P-C_{60} **2**, affiliated with Prototype I.

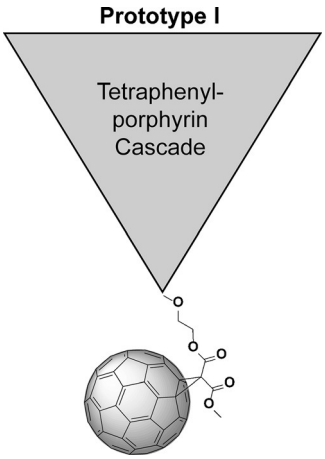

Figure 3. Prototype I (TPP–fullerene hybrids).

detail on these observations, in particular with respect to possible up–down permutations in such species.

Results and Discussion

Synthesis of Prototype I compounds

Firstly, we present the synthesis of ferrocene-containing Prototype I compound **2**. It has a large dendritic redox gradient, which starts at the nine ferrocene moieties (best donor), spans over the three zinc porphyrins and the free-base porphyrin, and ends at C_{60} (best acceptor). The nine ferrocene groups of compound **2** were introduced in the form of an aldehyde. A coupling reaction of ferrocenecarboxylic acid and 3-(2-hydroxyethoxy)benzaldehyde (**5**) gave 2-(3-formylphenoxy)ethyl ferrocenecarboxylate (**6**; Scheme 1).

The ferrocene aldehyde was used to synthesize the peripheral ferrocene porphyrins of compound **2**. Aldehyde **5** and aldehyde **6** were subjected to a Lindsey-type[16–21] condensation reaction with pyrrole, followed by metalation of the resulting porphyrin (Scheme 2). An alternative synthesis of porphyrin **7** can be found in the Supporting Information. Zinc porphyrin Fc_3-ZnP-OH **8** and dyad $(HOOC)_3$-H_2P-C_{60} **9**[15] were coupled in

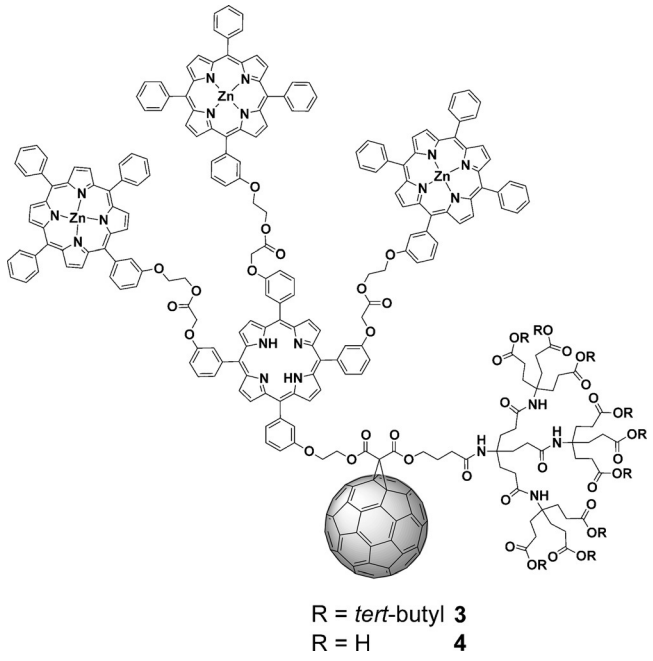

Figure 4. $(ZnP)_3$-H_2P-A2G-C_{60} **3** and deprotected compound **4**.

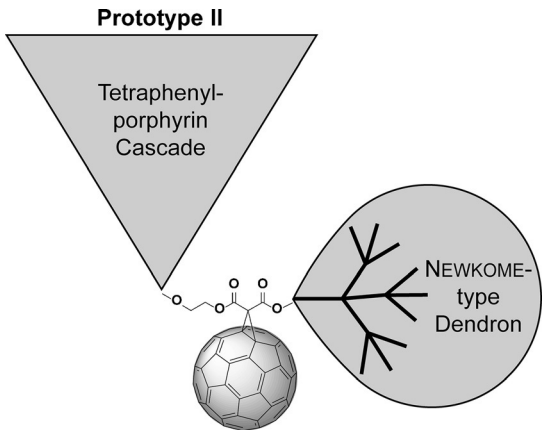

Figure 5. Prototype II (dendronized TPP–fullerene hybrids).

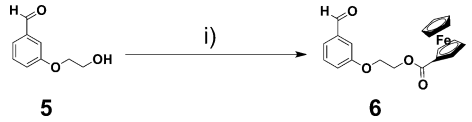

Scheme 1. Synthesis of aldehyde **6**. i) Ferrocenecarboxylic acid, DCC, CH_2Cl_2.

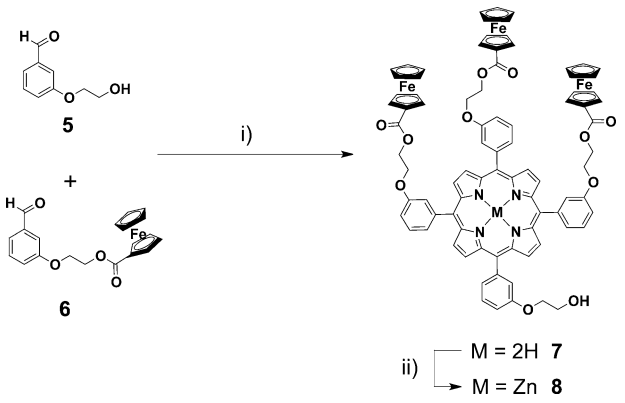

Scheme 2. Synthesis of ferrocene porphyrin **8**. i) Pyrrole, PPh_4Cl, EtOH, $BF_3{\cdot}Et_2O$, 2,3-dichloro-5,6-dicyano-1,4-benzoquinone (DDQ), CH_2Cl_2; ii) $Zn(OAc)_2{\cdot}2H_2O$, THF.

THF by using *N,N'*-dicyclohexylcarbodiimide (DCC), 1-hydroxybenzotriazole (HOBT), and 4-dimethylaminopyridine (DMAP; Scheme 3).

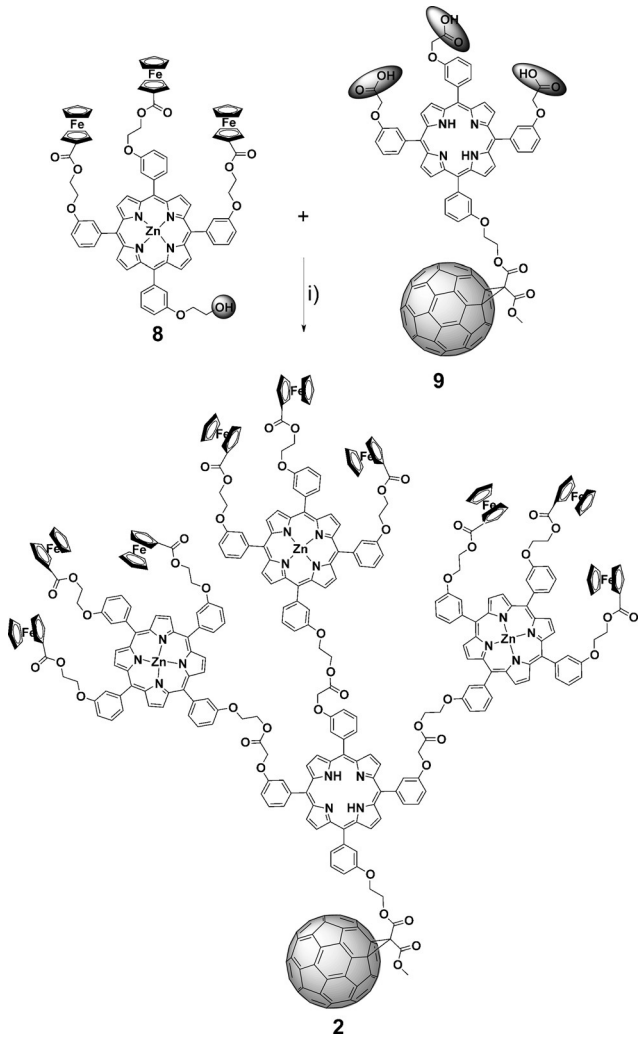

Scheme 3. Synthesis of Fc_9-$(ZnP)_3$-H_2P-C_{60} **2**. i) DCC, DMAP, 1-HOBt, THF.

The product Fc_9-$(ZnP)_3$-H_2P-C_{60} **2** was obtained in 66% yield by using well-established coupling reagents. Good solvents for DCC coupling reactions in our experience are THF and DMF. Reactions were monitored by TLC ($EtOAc/CH_2Cl_2$ 1/20). Three spots were observed on the TLC plate, corresponding to the product **2**, zinc porphyrin **8**, and dyad **9** at the baseline. Addition of 1 vol% NEt_3[22] to the mixture of eluting solvents helped only slightly to suppress peak tailing. According to experience, the best mode of operation for column chromatography of our compounds is gravity mode, although the dendritic TPP–fullerene hybrid Fc_9-$(ZnP)_3$-H_2P-C_{60} **2** can be separated from the precursor porphyrin **8** and dyad **9** by column chromatography. All dendritic compounds were obtained in chromatographically and spectroscopically pure form and were fully characterized (^1H NMR, ^{13}C NMR, IR, UV/Vis, elemental analysis, MALDI, and ESI-QIT and ESI-TOF MS). Even though aggregation and atropisomerism complicated the interpretation of the ^1H NMR and ^{13}C NMR spectra, high-resolution ESI mass spectra with fully resolved isotopic patterns support our structural assignments. MALDI-TOF-MS revealed $[MH]^+$ ($m/z = 6326$). ESI-QIT-MS showed $[M]^{3+}$ ($m/z = 2107.4$), $[M]^{4+}$ (1581.1), $[M]^{5+}$ (1265.2), and $[M]^{6+}$ (1054.5). ESI-TOF-HRMS gave evidence for $[M+2Na]^{2+}$ ($m/z = 3184.95901$), $[MH+Na]^{2+}$ (3173.96517), and $[MH_2]^{2+}$ (3162.47224). ESI-TOF-HRMS revealed peaks for $[M]^{3+}$ ($m/z = 2107.9754$), $[M]^{4+}$ (1581.2315), $[M]^{5+}$ (1264.7844), and $[M]^{6+}$ (1054.1538). The dendritic reference compound **10** (Figure 6) was synthesized similarly to compound **2**.

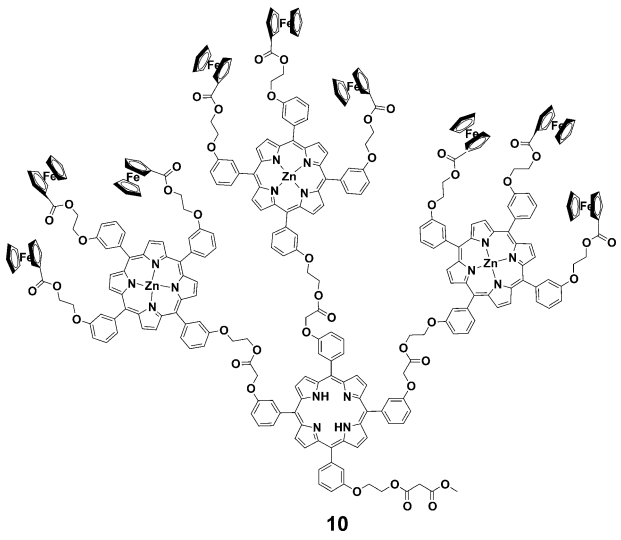

Figure 6. Fc_9-$(ZnP)_3$-H_2P **10**.

Synthesis of Prototype II compounds

In addition to the TPP cascade of the Prototype I compounds, the Prototype II compounds contain a Newkome-type dendron, covalently attached by a short linker. In its protected form (*tert*-butyl carboxylate end caps), the Newkome-type dendron enhances the solubility of the compounds in organic solvents. In its deprotected form (free carboxyl end caps), it can mediate pH-dependent water solubility. Our Prototype II com-

pounds can be divided into three parts, namely, the TPP cascade, the Newkome-type dendron, and the fullerene.

Firstly, we present the synthesis of the TPP cascade of the Prototype II compounds. The cascade contains one central free-base porphyrin and three peripheral zinc porphyrins. First, the aldehydes for the central porphyrin were synthesized. Treatment of 3-hydroxybenzaldehyde with benzyl 2-bromoacetate afforded aldehyde **11** (Scheme 4). Compound **5** was transformed into its *tert*-butyldiphenylsilyl (TBDPS)-protected derivative **12** (Scheme 5).

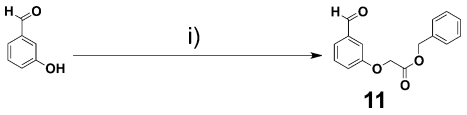

Scheme 4. Synthesis of aldehyde **11**. i) Benzyl 2-bromoacetate, tetra-*n*-butylammonium bromide (TBAB), NaOH, H_2O/CH_2Cl_2.

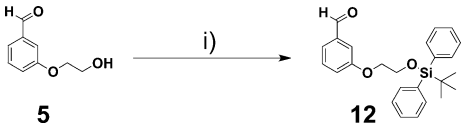

Scheme 5. Synthesis of aldehyde **12**. i) TBDPSCl, pyridine, CH_2Cl_2, DMAP.

Aldehydes **11** and **12** were subjected to a Lindsey-type condensation reaction with pyrrole, which gave porphyrin **13**. The latter was deprotected to give central porphyrin **14** (Scheme 6). An alternative synthesis of porphyrin **14** is provided in the Supporting Information. Focal porphyrin **14** was treated with TPP **15**[12] to obtain dendritic porphyrin **16**, which was deprotected to give TPP cascade **17** (Scheme 7).[23–25]

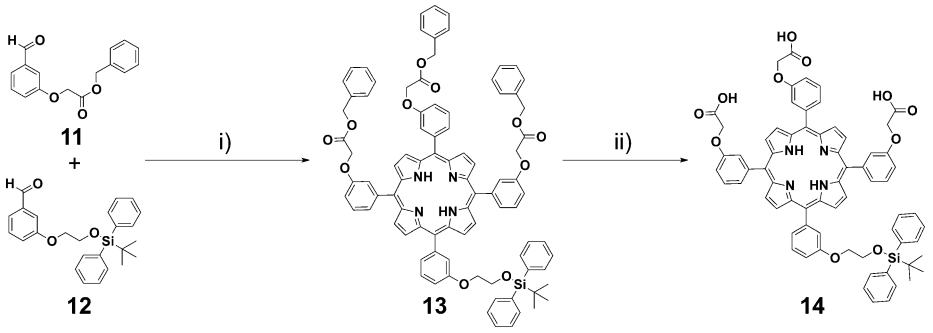

Scheme 6. Synthesis of central porphyrin $(HOOC)_3$-H_2P-OTBDPS **14**. i) Pyrrole, PPh_4Cl, EtOH, BF_3·Et_2O, DDQ, CH_2Cl_2; ii) K_2CO_3, THF/H_2O.

Consecutively, the Newkome-type compound for our Prototype II moieties was synthesized. Coupling of spacer **18**[26] and Newkome-type dendron **19**[27–29] was mediated by DCC and 1-HOBt in dry DMF to give derivative Bn-sp-A2G **20** (Bn = benzyl, sp = spacer, A2G = second-generation amine). The benzyl group of **20** was subsequently removed by catalytic hydrogenation (Pd/C) in EtOH to give **21** (Scheme 8). A malonyl group, which is needed for cyclopropanation of C_{60}, was introduced into compound **21** by malonic acid (Scheme 9). Polar EtOAc/MeOH mixtures were necessary in the column-chromatographic workup of free carboxylic acid **22**. Subsequent reactions of Newkome-type compound **22** can be used to build dendronized moieties. Coupling of **17** and **22** in dry DMF with DCC, DMAP, and 1-HOBt gave $(ZnP)_3$-H_2P-A2G **23** (Scheme 10). The yield of 24% is probably due to the sterically demanding entities. Cyclopropanation of $(ZnP)_3$-H_2P-A2G **23** was successful in toluene with C_{60}, iodine, and 1,8-diazabicyclo[5.4.0]undec-7-ene (DBU; Scheme 11).

Mild and reliable methods are required for the deprotection of $(ZnP)_3$-H_2P-A2G-C_{60} **3**. Acidic standard methods cannot be applied, because under these conditions the zinc cation can migrate from a ZnP to an H_2P. Deprotected fullerene adduct $(ZnP)_3$-H_2P-A2G-C_{60} **4** was gained from its precursor $(ZnP)_3$-H_2P-A_2G-C_{60} **3** by the use of Me_3SiOTf and 2,6-lutidine in dry CH_2Cl_2 followed by hydrolysis in H_2O (Scheme 12).[25,30–32] ESI-TOF-HRMS supported the structural assignments of **3** and **4**. The

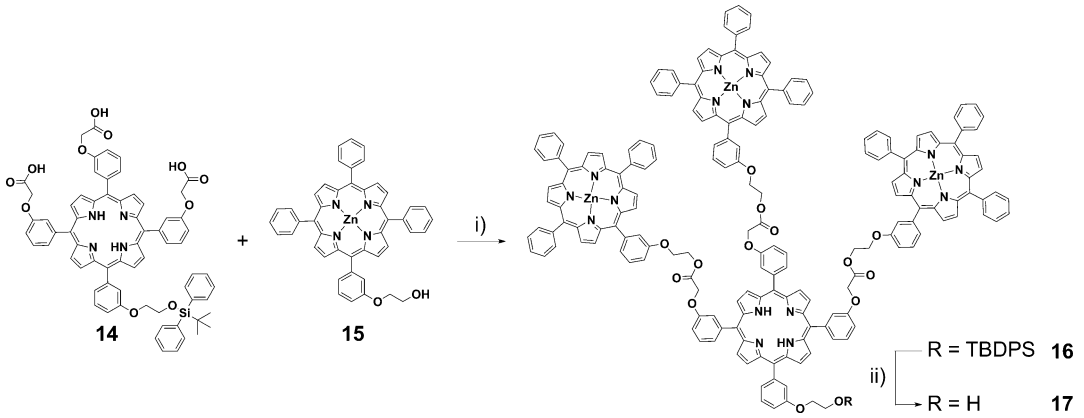

Scheme 7. Synthesis of dendritic TPP $(ZnP)_3$-H_2P-OH **17**. i) [*O*-(7-Azabenzotriazol-1-yl)-*N*,*N*,*N*′,*N*′-tetramethyluronium-hexafluorphosphate] (HATU), NEt_3, DMF; ii) TBAF, THF.

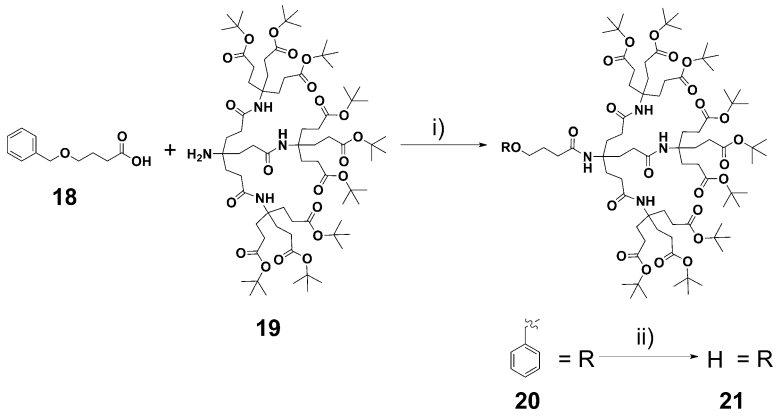

Scheme 8. Synthesis of Bn-sp-A2G **20** (A2G = second-generation amine) and HO-sp-A2G **21**. i) DCC, 1-HOBt, DMF; ii) H_2/Pd/C, EtOH.

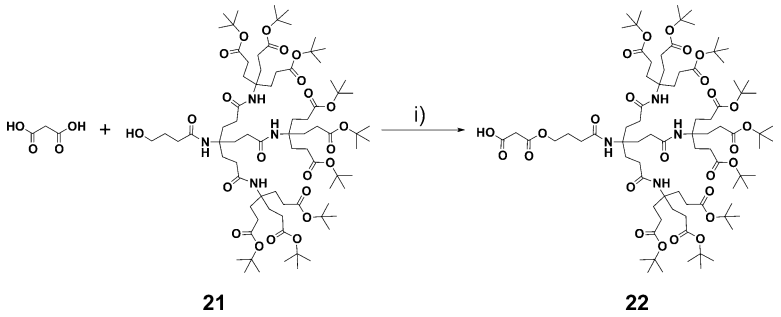

Scheme 9. Synthesis of **22**. i) DCC, CH_2Cl_2.

former gives rise to an isotopic pattern at $m/z = 2707.87052$, which was assigned to $[M+2\,Na]^{2+}$. The latter required treatment with NaOMe in MeOH to obtain a significant mass spectrum with peaks at $m/z = 2452.3$ $[M-4\,H+2\,Na]^{2-}$, 2442.3 $[M-3\,H+Na]^{2-}$, 2430.3 $[M-2\,H]^{2-}$, 1627.8 $[M-4\,H+Na]^{3-}$, and 1620.1 $[M-3\,H]^{3-}$.

Similarly to compound **4**, reference compound **24** was synthesized (Scheme 10). However, the deprotected compounds **4** and **24** were not soluble in water. This is due to the size of the Newkome-type dendron with its nine carboxyl groups. A higher-generation dendron should be used to achieve water solubility. A slight uptake of substance after intense sonication (20–60 min) was observed. This was judged by a slight color change of the solution, even though a solid residue remained. Because of the long sonication time, it must be assumed that decomposition of the porphyrins and the fullerene occurred. This assumption is supported by new bands in the UV region below 300 nm. It is known that fullerenes can be oxidized due to hydroxylation[33] and that malonic esters can be cleaved at pH 10.

The next synthetic targets were Prototype II compounds extended by ferrocene. Ferrocene porphyrin Fc_3-ZnP-OH **8** was treated with porphyrin **14** in a DCC coupling reaction in THF. Deprotection of the masked OH group of Fc_9-$(ZnP)_3$-H_2P-OTBDPS **25** could be achieved with

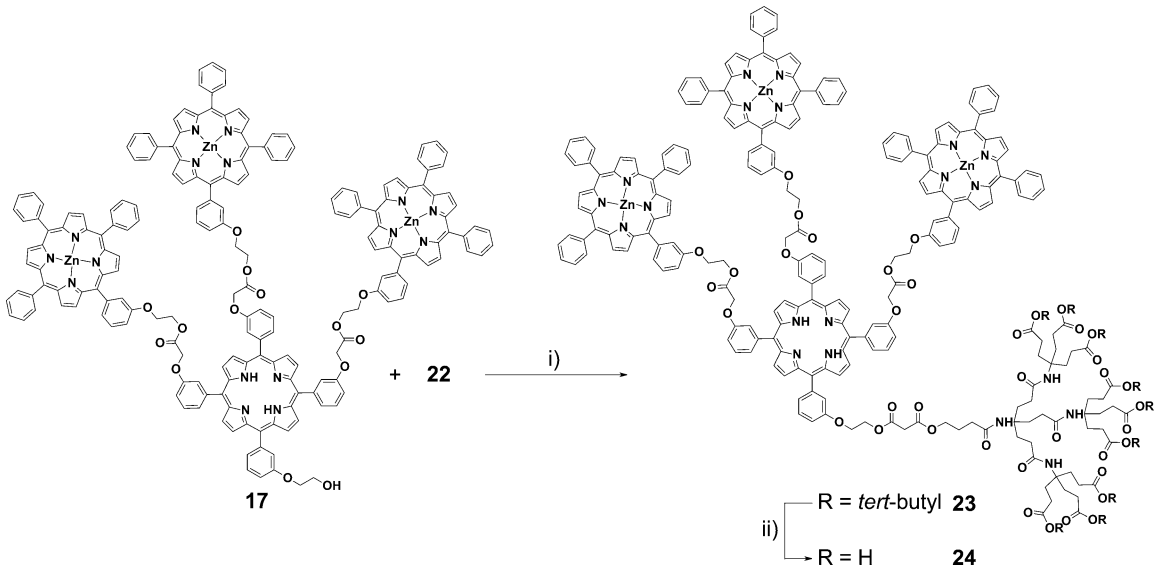

Scheme 10. Synthesis and deprotection of dendritic TPP $(ZnP)_3$-H_2P-A2G **23**. i) DCC, DMAP, 1-HOBt, DMF; ii) Me_3SiOTf, 2,6-lutidine, dry CH_2Cl_2.

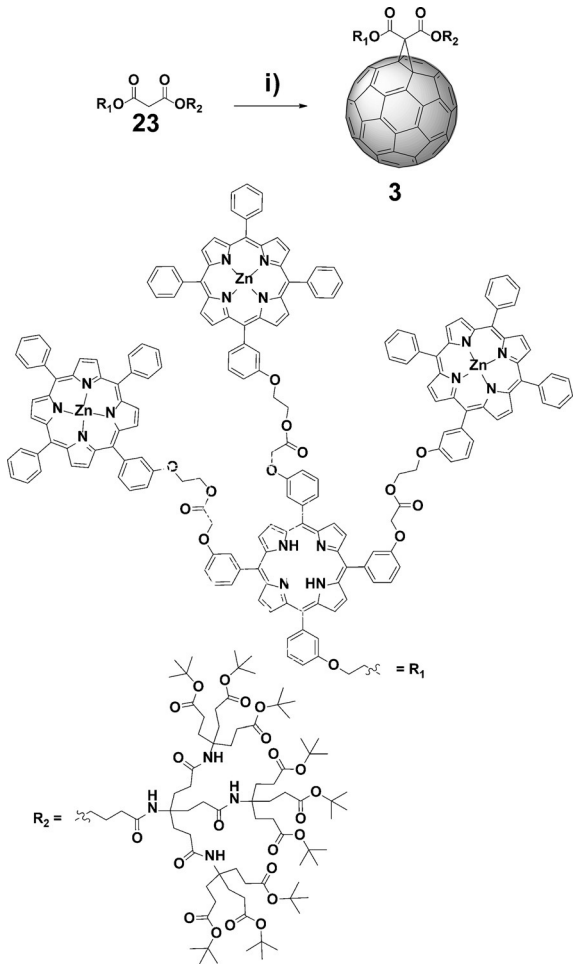

Scheme 11. Cyclopropanation of $(ZnP)_3$-H_2P-A2G **23**. i) C_{60}, I_2, DBU, toluene.

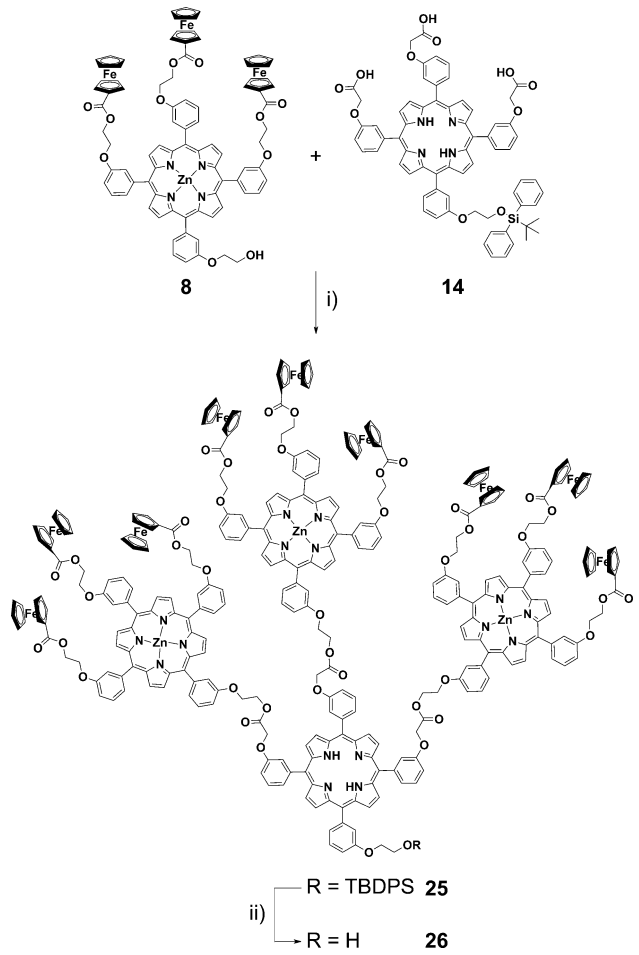

Scheme 13. Synthesis of dendritic ferrocene porphyrin **26**. i) DCC, DMAP, 1-HOBt, THF; ii) TBAF, THF.

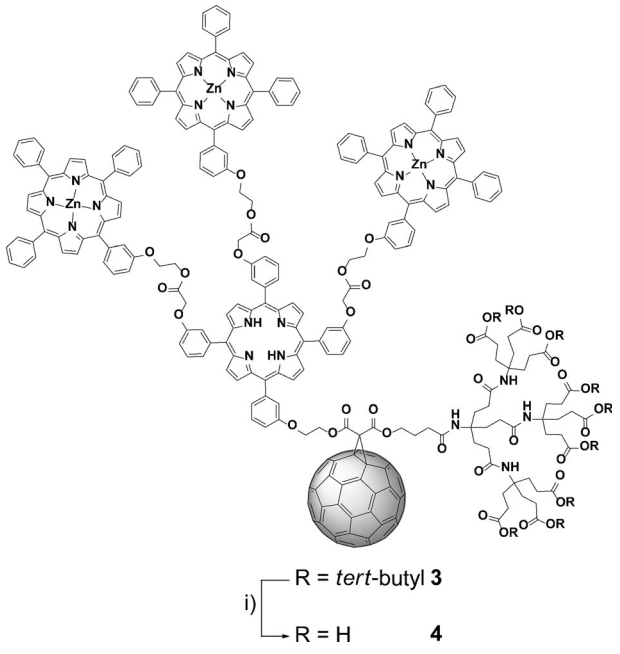

Scheme 12. Deprotection of fullerene adduct $(ZnP)_3$-H_2P-A2G-C_{60} **3**. i) Me_3SiOTf, 2,6-lutidine, dry CH_2Cl_2.

one equivalent of tetra-*n*-butylammonium fluoride (TBAF) in THF and furnished Fc_9-$(ZnP)_3$-H_2P-OH **26** (Scheme 13).[23–25]

Coupling of Newkome-type derivative **22** and dendritic ferrocene porphyrin **26** and was unsuccessful. Because of the limited amount of substance, not enough synthetic trials could be made. Thus, ferrocene-extended Prototype II compounds could not be synthesized. In addition, recent studies suggest that ferrocene may hamper energy and electron transfer in multicomponent scaffolds.[34]

Compounds **2** and **4** could be used as lead structures for rigid derivatives and derivatives which carry higher generation dendrons for mediation of water solubility.

Atropisomerism

Atropisomerism is well known in TPP chemistry, especially in *ortho*-functionalized TPPs. For example, Gottwald and Ullman 1969,[35] Walker and Avery 1971,[36] Drexler et al. 1998,[37] and Song et al. 1999[38] contributed to this topic. Collman and coworkers used atropisomerism in porphyrins to build picket-fence porphyrins to mimic heme-containing enzymes.[39,40] Porphyrins bearing bulky substituents in *meta* positions also exhibit atropisomerism. This was demonstrated by Smith and co-

workers in porphyrin–carborane systems,[41] by Nierengarten and Urbani in C_{60} porphyrin bis-adducts,[42] and by us in *trans*-2 C_{60} porphyrin bis-adducts.[13,14] Atropisomerism was also observed by NMR spectroscopy in linear bis([60]fullerene)–oligoporphyrin nanoarrays by Diederich and co-workers.[43,44] Herein, we report atropisomerism in dendritic tetraphenyl-porphyrins, which was observed by NMR spectroscopy. Analogous signals were previously reported in the case of much simpler porphyrins.[35–38]

TPPs are not flat like porphin (the porphyrin core), because the four phenyl rings, which are attached in *meso* positions, are oriented perpendicular to the porphyrin core. Consequently, there is only limited electronic communication between the phenyl substituents and the porphyrin core.[45–48] The rotational barrier for unsubstituted phenyl rings at room temperature is about 73 kJ mol^{-1}. For *ortho*-substituted rings the rotational barrier is even higher. The two facial sides of the porphyrin core become distinguishable if one phenyl ring has different substituents in *ortho* or *meta* position. Since the phenyl rings are perpendicular to the porphin plane, the substituents can be on one or the other side of this plane (α/β; Figure 7).

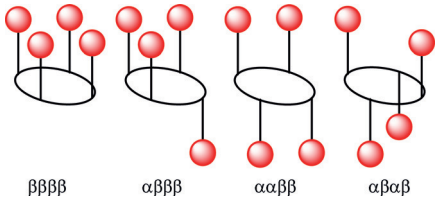

Figure 7. All possible TPP atropisomers bearing substituents above (β) and below (α) the porphyrin plane, for the case of identical substituents.

If all phenyl rings carry the same substituents at the same positions, four different isomers are possible. In the $\beta\beta\beta\beta$ isomer all substituents are on one side of the porphyrin. In the $\alpha\beta\beta\beta$ isomer, one substituent is on one side of the porphyrin and the other three are on the other side of the porphyrin. In the $\alpha\alpha\beta\beta$ isomer, two adjacent substituents are on one side of the porphyrin and two adjacent substituents are on the other side. In the $\alpha\beta\alpha\beta$ isomer, the substituents alternately are on one side and on the other side of the porphyrin.

It is helpful to discuss previous publications before describing the atropisomerism of our dendritic TPPs: Gottwald and Ullman (1969),[35] Walker and Avery (1971),[36] Drexler et al. (1998),[37] and Song et al. (1999).[38] In 1969 Gottwald and Ullman reported an early example of atropisomerism in TPPs.[35] They identified the four stereoisomers of an *ortho*-hydroxy substituted TPP. In 1971, Walker and Avery observed atropisomerism in an *ortho*-methyl substituted Ni TPP by ^{1}H NMR spectroscopy.[36] The atropisomerism in the investigated porphyrin was evidenced by a pattern of six signals with intensity ratio of 1:1:2:2:1:1, which was assigned to the four methyl groups. Each one of them is located in an *ortho* position of one of the four phenyl groups of the TPP. The hindered rotation of the phenyl groups, due to steric interaction between the *ortho*-methyl groups and the β-pyrrolic hydrogen

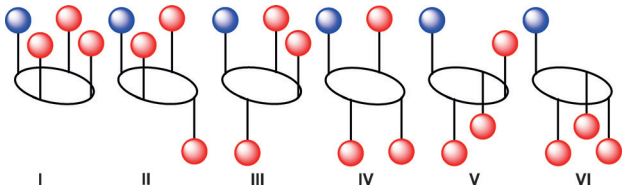

Figure 8. All six possible atropisomers emerging from an A_3B porphyrin (regarding dendritic porphyrin **27**; ellipse: H_2P plane, blue: methyl malonyl substituent, red: ZnP substituent). This figure also represents the six different chemical environments for one specific ligand in case of four identical ligands at the phenyl rings in TPPs.

atoms, enables four different isomers. There are six different chemical environments for the methyl group (Figure 8). This leads to the statistical occurrence of the isomers of 1:1:2:2:1:1. In fact, isomer III is a pair of enantiomers. Hence, it consists of two isomers, which are formed in equal amount, with identical physical properties and the same chemical shift. Consequently, it gives an NMR signal with twice the intensity compared to isomers I, II, V, and VI. The same is true for isomer IV, which is also a pair of enantiomers. The six isomers cause the six methyl signals observed in the ^{1}H NMR spectrum of the *ortho*-methyl-substituted Ni TPP. Drexler et al. (1998) synthesized a TPP bearing methyl-protected catecholamido groups in the *ortho* position and isolated all four atropisomers.[37] They identified the isomers with the help of NMR spectroscopy and X-ray diffraction. Song et al. synthesized *meso*-tetrakis(3-sulfonatomesityl)porphyrin tetrasodium salt and characterized its atropisomers in detail in a ^{1}H NMR study.[38] They analyzed the 1:1:2:2:1:1 pattern and assigned each of the six peaks to the corresponding atropisomer.

We were able to observe a similar pattern in our NMR spectra. Dendritic TPP **27**[15] (Figure 9) is discussed as a representative example of our dendritic porphyrins and TPP–fullerene hybrids, which all show to some degree signs of atropisomerism. The ^{1}H NMR spectrum of dendritic porphyrin **27**[15] at room temperature in $CDCl_3$ is shown in Figure 10. The building blocks of the molecule (ZnP, H_2P) can be recognized in the

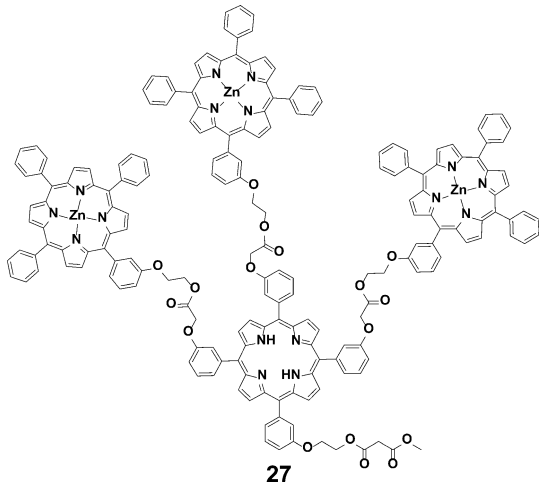

Figure 9. Dendritic TPP **27**.

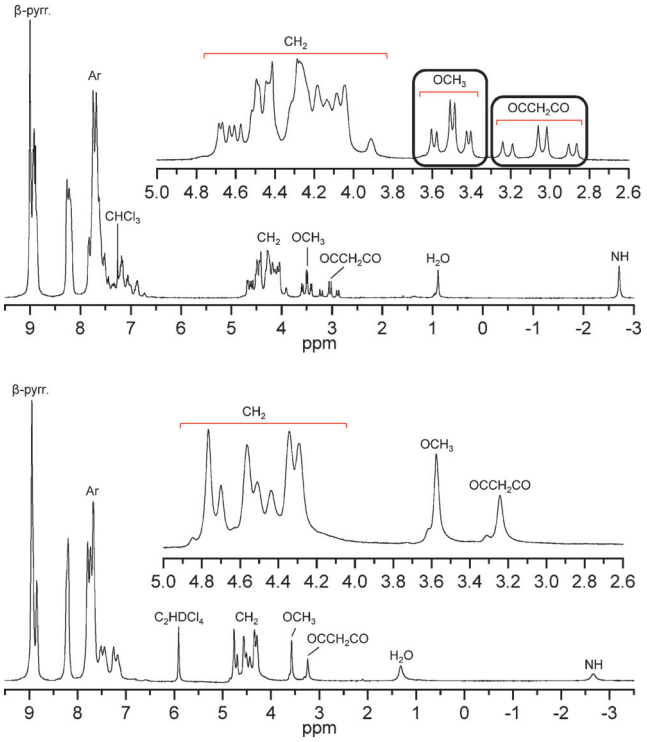

Figure 10. Top: ^{1}H NMR spectrum of $(ZnP)_3$-H_2P **27** (400 MHz, $CDCl_3$, RT). Bottom: ^{1}H NMR spectrum of $(ZnP)_3$-H_2P **27** (400 MHz, $C_2D_2Cl_4$, 100 °C).

^{1}H NMR spectrum of dendritic porphyrin **27**. Line broadening and signal overlap indicate a flexible molecule and various conformations. The most interesting feature are the resonances corresponding to the methyl malonic CH_2 group and the OCH_3 group. They were assigned to the two sets of six peaks between 2.8 and 3.7 ppm, each with an integral ratio of 1:1:2:2:1:1. Walker and Avery[36] described this pattern in 1971 for *ortho*-methyl substituted TPPs. Song et al.[38] (1999) assigned the single peaks in the 1:1:2:2:1:1 pattern of *meso*-tetrakis(3-sulfonatomesityl)porphyrin tetrasodium salt. We witnessed coalescence of the 1:1:2:2:1:1 pattern when we recorded a ^{1}H NMR spectrum of $(ZnP)_3$-H_2P **27** at high temperature (100 °C) in a high-boiling solvent ($C_2D_2Cl_4$; Figure 10, bottom). Therefore, we conclude that atropisomerism occurs in $(ZnP)_3$-H_2P **27**, which is a *meta*-substituted TPP.

Atropisomerism is common for *ortho*-substituted TPPs, but was also reported for *meta*-substituted TPPs with bulky substituents.[13,41,42] In our case, the three zinc porphyrins attached to the central free-base porphyrin are bulky substituents. Atropisomerism was not observed in the case of porphyrin **28** (Figure 11), which lacks the bulky ZnP substituents.

For the assignment, we propose the following hypothesis. Isomers VI to I (Figure 8) were assigned to the peaks of the 1:1:2:2:1:1 pattern (Figure 10). The most downfield peak corresponds to isomer VI, the next peak upfield to isomer V and so on up to the most upfield peak of the 1:1:2:2:1:1 pattern, which was assigned to isomer I. This correlation is based on the assumption of a shielding effect caused by the zinc porphyrins towards the methyl malonyl substituent if they are in close proximity to each other. This is only possible if they are

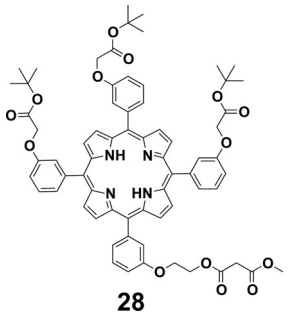

Figure 11. Porphyrin **28**.

on the same side of the plane of the free-base porphyrin. The shielding originates from the faces of the zinc porphyrins due to their aromatic ring current. The number and vicinity of zinc porphyrins to the methyl malonyl substituent increase from isomer VI to isomer I (Figure 8) in a corresponding way to the increasing shielding effect and chemical shift from isomer VI to isomer I. The single free-base porphyrin **28** can be used as a reference.

The shielding effect of the zinc porphyrin can be quantified and correlates very well with the distance of the methyl malonyl substituent to the zinc porphyrin in the individual atropisomers. In fact it is additive, that is, the number of zinc porphyrins in direct proximity to the methyl malonyl substituent is reflected by the chemical shift. In this way the patterns in the two sets of six singlets (3.60, 3.58, 3.51, 3.49, 3.42, 3.40 ppm and 3.24, 3.19, 3.06, 3.02, 2.90, 2.86 ppm; Figure 11, top) in the ^{1}H NMR spectrum of dendritic TPP **27** at room temperature in $CDCl_3$ can be rationalized.

If a ZnP substituent is added directly adjacent to the methyl malonyl substituent, for example, transformation of isomer VI into isomer IV, V into III, IV into II, or III into I, it causes an additional shift of 0.09 ppm to the corresponding signal of the methyl group. A second type of transformation is adding a ZnP substituent on the opposite side of the ring relative to the methyl malonyl substituent (isomer VI to isomer V, IV to III, or II to I). This causes an additional shift of 0.02 ppm to the corresponding signal of the methyl group. The corresponding set of six signals, which is assigned to the $OCCH_2CO$ group in the methyl malonyl substituent, can be treated in the same way. However, different additional shifts, that is, 0.18 to 0.16 ppm for a directly adjacent ZnP and 0.05 to 0.04 ppm for a ZnP on the opposite side of the ring, are observed.

The individual building blocks of $(ZnP)_3$-H_2P **27** can be recognized in its ^{13}C NMR spectrum (Figures 12 and 13). Compared to the signals of precursor porphyrins **15** and **28**, the signals of the dendritic TPP **27** are ragged. The pattern discussed for the ^{1}H NMR spectrum can also be recognized if the ^{13}C NMR resonances corresponding to the two malonyl carbonyl carbon atoms of **27** are considered.

The signals that are assigned to the two malonyl carbonyl carbon atoms can be observed around 166.3 ppm (166.56, 166.42, 166.30, 166.14, 166.04 ppm). The observed pattern in the ^{13}C NMR spectrum (Figure 12) is similar to the 1:1:2:2:1:1 pattern in the ^{1}H NMR spectrum (Figure 11). However, they are

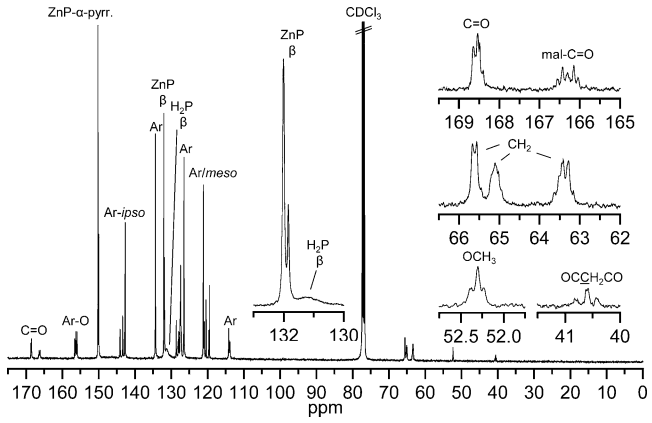

Figure 12. ^{13}C NMR spectrum of dendritic TPP **27** (100.5 MHz, $CDCl_3$, RT).

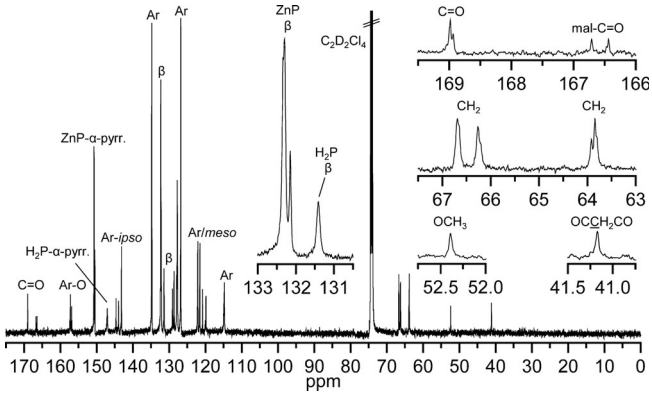

Figure 13. ^{13}C NMR spectrum of dendritic TPP **27** (100.5 MHz, $C_2D_2Cl_4$, 100 °C).

considered to be two unresolved sets of six singlets (corresponding to the two malonyl carbonyl carbon atoms), whereas the peak at 166.30 ppm is probably due to overlap of two peaks. A similar observation can be made if the OCH_3 and the $OCCH_2CO$ group of the methyl malonyl ligand are considered. In contrast to the split signals in the spectrum at room temperature (Figure 12), far fewer split signals are observed at 100 °C in $C_2D_2Cl_4$ (Figure 13). This is demonstrated by the CH_3 and CH_2 carbon atoms in the methyl malonyl group, which are detected in form of single peaks at 100 °C in $C_2D_2Cl_4$, and the two malonic carbonyl groups, which give rise to two individual peaks at 100 °C in $C_2D_2Cl_4$. The H_2P α-pyrrolic resonance at 147.06 ppm is detectable at 100 °C in $C_2D_2Cl_4$ but not at room temperature. The H_2P β-pyrrolic signal at 131.41 ppm, which is observed as a weak broad peak at room temperature, gives rise to a sharp peak at 100 °C in $C_2D_2Cl_4$.

We witnessed atropisomerism for every dendritic multiporphyrin moiety, the TPP–fullerene hybrids, and the single TPPs. For example, in the case of the single ferrocene porphyrins, a characteristic pattern was observed in spectra of concentrated solutions. On dilution or heating, assignable NMR spectra could be obtained in suitable solvents.

Conclusion

Several flexible, linked dendritic TPPs and TPP–fullerene compounds of Prototypes I and II were synthesized. These structures have a dendritic redox gradient along a porphyrin cascade. Additionally, the Prototype II compounds bear a Newkome-type dendron, which could be successfully transformed into its free carboxyl form by a mild procedure. The 1:1:2:2:1:1 pattern observed in the NMR spectra of the dendritic TPPs has been discussed and is ascribed to atropisomerism of the central TPP (H_2P) of the dendritic moieties.

Experimental Section

For experimental details, see Supporting Information.

Acknowledgements

Financial support by the German Science Foundation (DFG) through SFB 583 is gratefully acknowledged.

Keywords: atropisomerism · dendrons · fullerenes · metallocenes · porphyrinoids

[1] K. Tamaki, H. Imahori, Y. Sakata, Y. Nishimura, I. Yamazaki, *Chem. Commun.* **1999**, 625 – 626.
[2] H. Imahori, K. Tamaki, H. Yamada, K. Yamada, Y. Sakata, Y. Nishimura, I. Yamazaki, M. Fujitsuka, O. Ito, *Carbon* **2000**, *38*, 1599 – 1605.
[3] C. Luo, D. M. Guldi, H. Imahori, K. Tamaki, Y. Sakata, *J. Am. Chem. Soc.* **2000**, *122*, 6535 – 6551.
[4] H. Imahori, D. M. Guldi, K. Tamaki, Y. Yoshida, C. Luo, Y. Sakata, S. Fukuzumi, *J. Am. Chem. Soc.* **2001**, *123*, 6617 – 6628.
[5] H. Imahori, K. Tamaki, Y. Araki, Y. Sekiguchi, O. Ito, Y. Sakata, S. Fukuzumi, *J. Am. Chem. Soc.* **2002**, *124*, 5165 – 5174.
[6] H. Imahori, *Org. Biomol. Chem.* **2004**, *2*, 1425 – 1433.
[7] D. M. Guldi, I. Zilbermann, G. Anderson, A. Li, D. Balbinot, N. Jux, M. Hatzimarinaki, A. Hirsch, M. Prato, *Chem. Commun.* **2004**, 726 – 727.
[8] D. Kuciauskas, P. A. Liddell, S. Lin, T. E. Johnson, S. J. Weghorn, J. S. Lindsey, A. L. Moore, T. A. Moore, D. Gust, *J. Am. Chem. Soc.* **1999**, *121*, 8604 – 8614.
[9] M. S. Choi, T. Aida, H. Luo, Y. Araki, O. Ito, *Angew. Chem. Int. Ed.* **2003**, *42*, 4060 – 4063; *Angew. Chem.* **2003**, *115*, 4194 – 4197.
[10] E. Dietel, A. Hirsch, E. Eichhorn, A. Rieker, S. Hackbarth, B. Röder, *Chem. Commun.* **1998**, 1981 – 1982.
[11] F. Spänig, M. Ruppert, J. Dannhäuser, A. Hirsch, D. M. Guldi, *J. Am. Chem. Soc.* **2009**, *131*, 9378 – 9388.
[12] C. Kovacs, A. Hirsch, *Eur. J. Org. Chem.* **2006**, 3348 – 3357.
[13] M. Ruppert, F. Spänig, M. Wielopolski, C. M. Jäger, W. Bauer, T. Clark, A. Hirsch, D. M. Guldi, *Chem. Eur. J.* **2010**, *16*, 10797 – 10807.
[14] M. Ruppert, W. Bauer, A. Hirsch, *Chem. Eur. J.* **2011**, *17*, 8714 – 8725.
[15] S. Schlundt, G. Kuzmanich, F. Spänig, G. de Miguel Rojas, C. Kovacs, M. A. Garcia-Garibay, D. M. Guldi, A. Hirsch, *Chem. Eur. J.* **2009**, *15*, 12223 – 12233.
[16] A. D. Adler, F. R. Longo, W. Shergalis, *J. Am. Chem. Soc.* **1964**, *86*, 3145 – 3149.
[17] J. S. Lindsey, R. W. Wagner, *J. Org. Chem.* **1989**, *54*, 828 – 836.
[18] J. S. Lindsey, I. C. Schreiman, H. C. Hsu, P. C. Kearney, A. M. Marguerettaz, *J. Org. Chem.* **1987**, *52*, 827 – 836.
[19] J. S. Lindsey, K. A. MacCrum, J. S. Tyhonas, Y. Y. Chuang, *J. Org. Chem.* **1994**, *59*, 579 – 587.
[20] F. Li, Y. Kexin, J. S. Tyhonas, K. A. MacCrum, J. S. Lindsey, *Tetrahedron* **1997**, *53*, 12339 – 12360.
[21] G. R. Geier III, B. J. Littler, J. S. Lindsey, *J. Chem. Soc. Perkin Trans. 2* **2001**, 712 – 718.

[22] J. W. Dolan, *LCGC North Am.* **2003**, *21*, 612 – 616.
[23] Z. Yao, J. Bhaumik, S. Dhanalekshmi, M. Ptaszek, P. A. Rodriguez, J. S. Lindsey, *Tetrahedron* **2007**, *63*, 10657 – 10670.
[24] T. Yamaguchi, T. Kimura, H. Matsuda, T. Aida, *Angew. Chem. Int. Ed.* **2004**, *43*, 6350 – 6355; *Angew. Chem.* **2004**, *116*, 6510 – 6515.
[25] T. W. Greene, P. G. M. Wuts, *Protective Groups in Organic Synthesis*, 3rd ed., Wiley, New York, **1999**.
[26] M. Braun, S. Atalick, D. M. Guldi, H. Lanig, M. Brettreich, S. Burghardt, M. Hatzimarinaki, E. Ravanelli, M. Prato, R. van Eldik, A. Hirsch, *Chem. Eur. J.* **2003**, *9*, 3867 – 3875.
[27] G. R. Newkome, R. K. Behera, C. N. Moorefield, G. R. Baker, *J. Org. Chem.* **1991**, *56*, 7162 – 7167.
[28] G. R. Newkome, C. D. Weis, *Org. Prep. Proced. Int.* **1996**, *28*, 495 – 498.
[29] M. Brettreich, A. Hirsch, *Synlett* **1998**, 1396 – 1398.
[30] M. Duan, L. A. Paquette, *Angew. Chem. Int. Ed.* **2001**, *40*, 3632 – 3636; *Angew. Chem.* **2001**, *113*, 3744 – 3748.
[31] A. Trzeciak, W. Bannwarth, *Synthesis* **1996**, 1433 – 1434.
[32] M. Sakaitani, Y. Ohfune, *J. Org. Chem.* **1990**, *55*, 870 – 876.
[33] N. O. Mchedlov-Petrossyan, *Chem. Rev.* **2013**, *113*, 5149 – 5193.
[34] A. Kremer, E. Bietlot, A. Zanelli, J. M. Malicka, N. Armaroli, D. Bonifazi, *Chem. Eur. J.* **2015**, *21*, 1108 – 1117.
[35] L. K. Gottwald, E. F. Ullman, *Tetrahedron Lett.* **1969**, *10*, 3071 – 3074.
[36] F. A. Walker, G. L. Avery, *Tetrahedron Lett.* **1971**, *12*, 4949 – 4952.
[37] C. Drexler, M. W. Hosseini, J.-M. Planeix, G. Stupka, M. W. Hosseini, J.-M. Planeix, A. D. Cian, J. Fischer, *Chem. Commun.* **1998**, 689 – 690.
[38] R. Song, A. Robert, J. Bernadou, B. Meunier, *Analusis* **1999**, *27*, 464 – 467.
[39] J. P. Collman, *Acc. Chem. Res.* **1977**, *10*, 265 – 272.
[40] J. P. Collman, R. A. Decreau, C. Zhang, *J. Org. Chem.* **2004**, *69*, 3546 – 3549.
[41] M. G. H. Vicente, D. J. Nurco, S. J. Shetty, C. J. Medforth, K. M. Smith, *Chem. Commun.* **2001**, 483 – 484.
[42] M. Urbani, J.-F. Nierengarten, *Tetrahedron Lett.* **2007**, *48*, 8111 – 8115.
[43] D. Bonifazi, F. Diederich, *Chem. Commun.* **2002**, 2178 – 2179.
[44] D. Bonifazi, G. Accorsi, N. Armaroli, F. Song, A. Palkar, L. Echegoyen, M. Scholl, P. Seiler, B. Jaun, F. Diederich, *Helv. Chim. Acta* **2005**, *88*, 1839 – 1884.
[45] P. G. Gassman, A. Ghosh, J. Almlof, *J. Am. Chem. Soc.* **1992**, *114*, 9990 – 10000.
[46] A. Ghosh, *J. Mol. Struct.* **1996**, *388*, 359 – 363.
[47] T. Vangberg, A. Ghosh, *J. Am. Chem. Soc.* **1998**, *120*, 6227 – 6230.
[48] L. Jaquinod in *The Porphyrin Handbook, Vol. 1* (Eds.: K. M. Kadish, K. M. Smith, R. Guilard), **2000**, p. 226.

Received: March 30, 2015
Published online on July 31, 2015